ChemistrySelect

Research Article
doi.org/10.1002/slct.202301643

Chemistry Europe
European Chemical Societies Publishing

www.chemistryselect.org

Synthesis of Modified River Clay Catalyst for Valuable BTE Production via Catalytic Pyrolysis of Hazardous Plastic Waste

Anjali Verma[a] and Hiralal Pramanik*[a]

In the present study, silica-alumina rich river clay calcined at different temperatures are used as low cost natural green catalyst for the production of valuable aromatics benzene, toluene and ethylbenzene (BTE) via multiphase/Mp-type catalytic pyrolysis of waste expanded polystyrene (WEPS). The calcined river clay catalysts are designated as RHC-600, RHC-700, RHC-800 and RHC-900 after calcination at the temperature of 600 °C, 700 °C, 800 °C, and 900 °C, respectively. Whereas, the natural river harvested clay is designated as RHC. The RHC-800 catalyst is found to be the best catalyst for the WEPS pyrolysis due to its highest surface area of 18.83 m^2/g and high silica to alumina (Si/Al) ratio of 2.23 among all other river harvested clay catalysts. The styrene content get reduced from 84.74 wt.% to 65.30 wt.% and BTE content increased from 11.38 wt.% to 23.51 wt.% when the process is switched over from thermal to Mp-type catalytic pyrolysis using RHC-800 catalyst. The promising results of RHC-800 indicate that it can be an alternative to commercial catalyst for pyrolysis applications.

Introduction

Plastics are primarily derived from petroleum products.[1] The excellent properties of plastics such as high strength to weight ratio, electrical insulation, high durability, ductility, corrosion resistance, stiffness and toughness increases its applications in various fields i.e., electronics, textile, building and construction, and packaging.[2] However, the highest consumption of plastics (44%) is in the packaging field.[3] Due to the non-biodegradable nature[4] and wide range of applications, plastic has become a chief component of municipal solid waste (MSW).[5] Polyethylene (PE), polypropylene (PP), and polystyrene (PS) are the main components of plastic solid waste (PSW).[6]

The expanded polystyrene (EPS) is a light weight cellular thermoplastic used for insulation and packaging due to its excellent insulating and shock-absorbing properties.[7] The dimension stability, low cost, cleanliness and versatility of EPS make it suitable for industrial applications.[8] In addition, global EPS production is steadily increasing.[9] Although, EPS is a more common litter widespread worldwide in marine and freshwater environments.[10] Moreover, WEPS contributes 10 wt.% of the total municipal plastic waste, but by volume, it could be 40%.[11] Thus, the management of waste obtained from EPS is necessary because of its heavy disposal from industries and households.

The pyrolysis is a versatile method to minimize plastic waste because it offers various advantages over other recycling processes such as, pyrolysis converts the plastic waste into useful products i.e., solid residue, oil and combustible gases in a cleaner way.[12] The pyrolysis process requires a lower process temperature as compared to combustion. Moreover, the scale of pyrolysis plants is more flexible than incineration plants.[13] The heating of organic material at a moderate temperature (400–700 °C) in the inert atmosphere is known as pyrolysis.[14] Pyrolysis process can be accomplished in the presence of catalyst and without catalyst for catalytic pyrolysis and thermal pyrolysis, respectively. Although, thermal pyrolysis has become obsolete because of high energy consumption and non-selective product formation.[15]

The incorporation of a catalyst in the pyrolysis process offers various benefits over pure thermal pyrolysis, such as it reduces the temperature required for reaction by taking down the activation energy and favours the production of selective or target products.[16] In addition, the catalyst enhances plastic conversion and produces a narrower product distribution.[17] Various catalysts such as ZSM-5,[18] MCM-41,[19] HZSM-5,[19] FCC,[20] Y-zeolite,[21] HY-zeolite,[22] Hβ-zeolite,[22] USY-zeolite,[23] HUSY-zeolite,[24] β-zeolite[25] have been used for the pyrolysis process for the production of fuel range hydrocarbons.

The commercial catalysts are expensive and can have a relatively short life in a pyrolysis process.[26] Thus, there is a huge scope of utilizing low cost natural catalysts to achieve economic benefits in the pyrolysis process. Kyaw and Hmwe[27] used bentonite clay, mabisan clay, shwedaung clay and dolomite as the catalyst for the pyrolysis of mixed plastic waste in the temperature range of 32 °C-380 °C and found that the natural catalysts have good cracking efficiency due to their chemical components mainly silica and alumina. Similarly, Gaurh and Pramanik[28] conducted the pyrolysis of polyethylene in the temperature range of 500 °C-800 °C. The catalyst synthesized from fly ash was used to obtain the target molecules benzene, toluene, ethylbenzene and xylene (BTEX). The highest BTEX content of 22.10 wt.% was obtained using fly ash calcined at a calcination temperature of 800 °C i.e., FA-800 catalyst at a

[a] A. Verma, H. Pramanik
Department of Chemical Engineering and Technology, Indian Institute of Technology (Banaras Hindu University), Varanasi, India
E-mail: hpramanik.che@iitbhu.ac.in

Supporting information for this article is available on the WWW under https://doi.org/10.1002/slct.202301643

reaction temperature of 700 °C. Thus, the natural catalyst is also efficient to obtain valuable chemicals and fuel, as commercial catalysts.

It is already mentioned in the literature, thermal pyrolysis of PS mainly produced monomer styrene and styrene like compounds.[29] In addition, styrene is easily recovered from the pyrolysis of polystyrene due to its low activation energy. However, the pyrolysis of PS in the presence of acid catalyst produces more benzene, toluene and ethylbenzene (BTE) other than styrene as compared to thermal pyrolysis.[30] The Bronsted acid sites of acid catalyst are responsible for the formation of useful aromatics BTE.[31] On the other side, the Bronsted acidity of clays makes it scientifically and technically more important and thus, extensively used as acid catalysts in the oil refining and petrochemical industry.[32] The natural clays are generally composed of crystalline aluminosilicates layers superimposed on interlayers of hydrated ions. The non-toxic solid clay catalysts can catalysed the various organic reactions such as hydrogenation, alkylation, isomerization, and cyclization.[33]

So far, no such work on river clay synthesized catalyst for polystyrene pyrolysis has been reported in open literature. In this context, green catalyst synthesized from natural river clay has been used for the pyrolysis of WEPS to produce valuable aromatics BTE in the present study. The valuable aromatic hydrocarbons BTE are used in various chemical and petrochemical industries as raw materials.[34] Benzene is majorly used for manufacturing industrial chemicals, explosives and solvents for resins, waxes, oil and natural rubber.[35] Toluene also has various industrial and commercial applications, such as precursor for the production of benzene, xylene, toluene diisocyanate for manufacturing the trinitrotoluene and polyurethane foam.[36] Ethylbenzene is mostly used for styrene production, which is then used for the production of variety of polymers such as polystyrene (PS), styrene acrylonitrile, acrylonitrile butadiene styrene and other products.[37] Apart from this, BTE are added to gasoline to improve the octane rating.[38,39] As per reported literature, the monomer styrene is also obtained in an adequate amount from the catalytic pyrolysis of polystyrene. Thus, styrene can be separated from the pyrolysis oil and stored after adding the polymerization inhibitors because of its rapid polymerization nature.[40]

In this study, the catalytic pyrolysis of WEPS in three different reactor arrangements i.e., liquid phase/Lp-type, vapour phase/Vp-type and multiphase/Mp-type has been investigated. The river clay synthesized catalyst was used in the present study, keeping in mind that the undesired styrene should be as low as possible in the pyrolysis oil. The various pyrolysis parameters such as feed to catalyst ratio, heating rate and temperature were optimized to produce the maximum liquid yield with better quality in terms of BTE content.

Results and discussion

Catalyst characterization

X-ray diffraction (XRD) analysis

The ubiquitous clay minerals have acidic sites, high adsorption capacity, and ion exchange capability, making them suitable for application as a catalyst in various processes.[41] The XRD analysis verified the presence of clay minerals and their various forms in raw and calcined river harvested clay catalysts. Figure 1a–e shows the XRD pattern of natural and calcined river harvested clay catalysts i.e., RHC, RHC-600, RHC-700, RHC-800 and RHC-900, respectively. It is clear from the XRD pattern of RHC catalyst (Figure 1a) the raw river harvested clay (RHC) was mainly composed of kaolinite ($Al_2Si_2O_5$ $(OH)_4$), illite and micas and α-quartz. It is also seen from Figure 1a that the peaks of illite and micas were observed at $2\theta = 8.89°$, 17.80°, and 19.82° corresponding to the basal spacing of d = 9.94 Å, 4.98 Å, and 4.48 Å, respectively. The peaks related to kaolinite were observed at $2\theta = 36.02°$ and 37.70° corresponding to the basal spacing of d = 2.49 Å and 2.38 Å, respectively.[42] Whereas, the, intense peaks of α-quartz were observed at $2\theta = 20.85°$, 26.64°, 39.48°, 40.30°, 42.47°, 50.15°, 54.90°, 64.05°, 68.16°, 68.31° and 75.67° corresponding to the d = 4.26 Å, 3.34 Å, 2.28 Å, 2.24 Å, 2.13 Å, 1.82 Å, 1.67 Å, 1.45 Å, 1.38 Å, 1.37 Å and 1.26 Å, respectively (JCPDS 5–490). Figure 1b shows the XRD spectra of the river harvested clay calcined at a temperature of 600 °C (RHC-600). It should be noted from Figure 1b that the peaks related to kappa alumina at $2\theta = 19.65°$, 29.42° corresponding to the d = 4.51 Å, 3.03 Å, respectively were also observed along with α-quartz, kaolinite and illite and micas. The additional peak related to the delta alumina (at $2\theta = 34.46°$ corresponding to the d = 2.60 Å) was observed in the XRD pattern of RHC-700 catalyst (Figure 1c). However, the peak related to the kaolinite was completely diminished, which confirms the complete transformation of kaolinite into metakaolinite via dehydroxylation process at the calcination temperature of 700 °C.

The dehydroxylation is a reaction of decomposition of kaolinite crystals to a partially disordered structure which have higher porosity.[43] Nmiri et al.[44] also reported the metakaolin formation with highest reactivity at a temperature of 700 °C. Furthermore, the calcination process at the high temperature promotes the formation of transition alumina such as kappa alumina, delta alumina, and theta alumina which have excellent catalytic and adsorptive properties.[45] Thus, XRD pattern of RHC-800 (Figure 1d) shows the peaks related to all possible transition aluminas. The peaks related to transition alumina i.e., kappa, delta and theta alumina were verified with ICDD 16–0394, ICDD 16–0394 and ICDD 10–0425, respectively. Figure 1d shows the peaks related to the κ-kappa alumina at $2\theta = 19.64°$, 50.09° corresponding to the d = 4.52 Å and 1.82 Å, respectively. The peaks related to the delta alumina were observed at $2\theta = 27.63°$ and 31.10° corresponding to the d = 3.23 Å and 2.87 Å, respectively. The peaks related to one more transition alumina i.e., theta alumina were also observed at $2\theta = 36.90°$, 44.97° corresponding to the d = 2.43 Å and 2.01 Å, respectively.

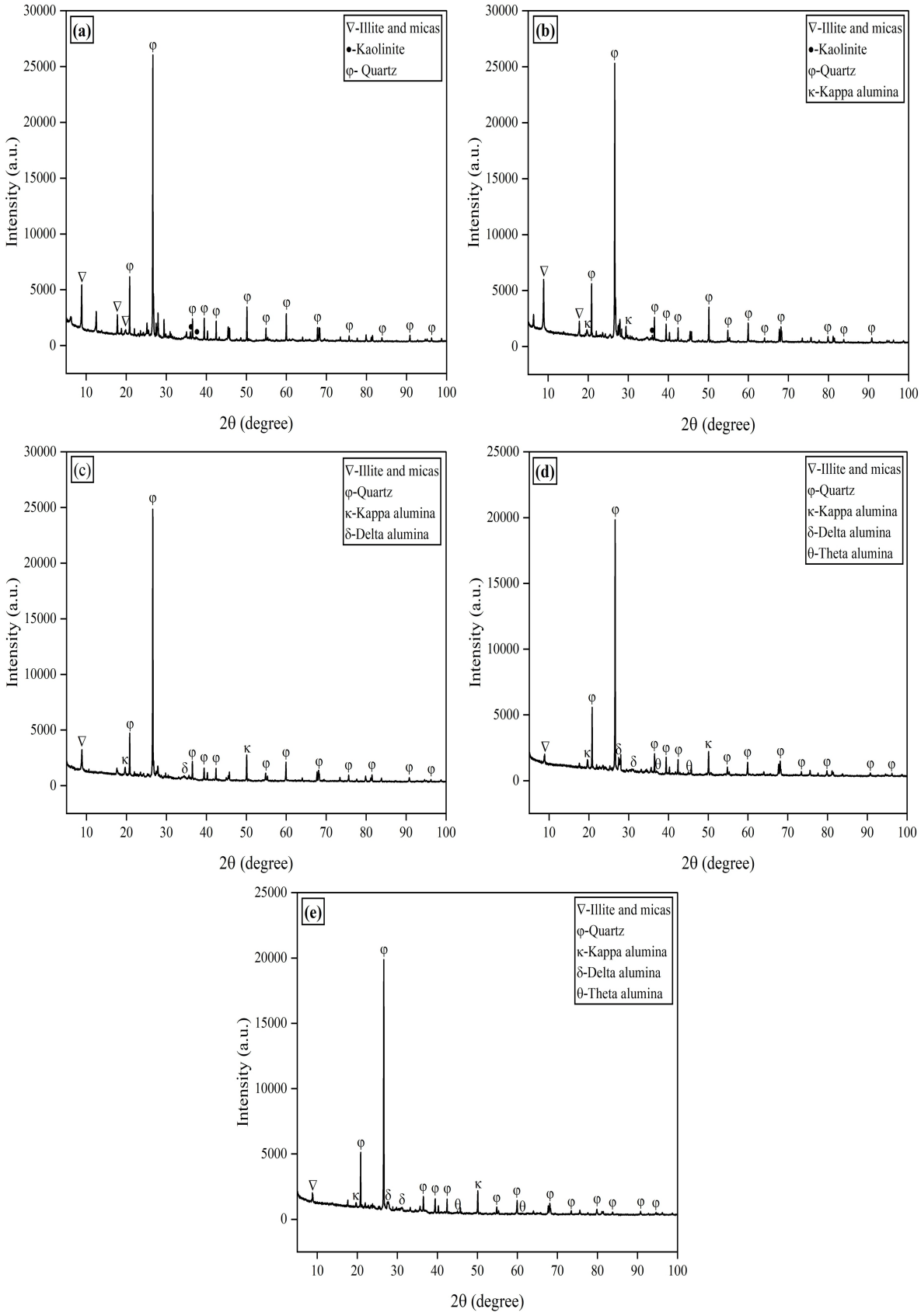

Figure 1. XRD analysis of river harvested clay (a) raw river harvested clay (b) river clay calcined at 600 °C (c) river clay calcined at 700 °C (d) river clay calcined at 800 °C (e) river clay calcined at 900 °C.

Similarly, the XRD pattern of RHC-900 (Figure 1e) shows the peaks related to the kappa alumina at $2\theta = 19.70°$, 50.10° corresponding to the d = 4.50 Å and 1.82 Å, respectively. The peak related to the delta and theta alumina were observed at $2\theta = 27.77°$ corresponds to d = 3.21 Å and $2\theta = 45.04°$ corresponds to d = 2.01 Å, respectively. Furthermore the intense peak related to quartz at $2\theta = 26.64°$ corresponding to the d = 3.34 Å was observed for all river clay synthesized catalysts (Figure 1a–e).

Scanning electron microscopy-energy dispersive X-ray (SEM-EDX) analysis

The captured SEM images of raw river harvested clay (RHC), river clay calcined at 600 °C (RHC-600), river clay calcined at 700 °C (RHC-700), river clay calcined at 800 °C (RHC-800) and river clay calcined at 900 °C (RHC-900) river harvested clay catalysts showing morphological transformations upon calcination are reported in Figure 2a–e, respectively.

Figure 2a illustrates the morphology of raw river harvested clay containing flakes of different size. The structure turns to irregular and porous when river clay calcined from 600 °C to 800 °C (Figure 2b–d). However, not much significant difference was observed between the morphology of raw river clay and river clay calcined at temperature up to 700 °C (Figure 2a–c). Furthermore, the structure of river harvested clay calcined at 900 °C became very dense due to the pore blockage because of the sintering phenomenon.[46] The structure of river clay calcined at 800 °C (Figure 2d) was more flaky and porous in nature as compared to other river harvested clay catalysts. The elemental composition determined by EDX analysis of river harvested clay catalysts i.e., RHC, RHC-600, RHC-700, RHC-800 and RHC-900 are given in Table 1 and corresponding EDX figures are also given in Figure S4 (a–e). As it is reported in the literature, the high Si/Al ratio is directly related to the acidity of catalyst, which means higher the Si/Al ratio, higher the acidity of catalyst.[47] It is seen from the Table 1 that the Si/Al ratio increases from 1.20 to 2.23 with the increase in calcination temperature from 600 °C to 800 °C. It may be due the formation of relatively more porous structure with the increase in calcination temperature from 600 °C to 800 °C (Figure 2a–d).[28]

The BET surface area analysis also shows the highest surface area for the calcination temperature of 800 °C. Thus, the highest Si/Al ratio of 2.23 was observed at a calcination temperature of 800 °C (Figure 2d). However, the river clay calcined beyond the temperature 800 °C i.e., RHC-900 came up with the lower Si/Al ratio of 1.23 and it may be due to the pore blockage because of sintering phenomenon.[46] The blocked pores of RHC-900 catalyst can also observed in SEM image of RHC-900 catalyst (Figure 2e).

Nitrogen adsorption/desorption curve and Brunauer Emmett Teller (BET) surface area

The nitrogen adsorption/desorption curve of river harvested clay catalysts i.e., raw river clay (RHC), river clay calcined at 600 °C (RHC-600), river clay calcined at 700 °C (RHC-700), river clay calcined at 800 °C (RHC-800) and river clay calcined at 900 °C (RHC-900), presented in Figure 3a–e, respectively. The synthesized river clay catalysts i.e., RHC, RHC-600, RHC-700, RHC-800 and RHC-900 show the type-IV isotherm.[48] Type-IV isotherm confirms the mesoporous structure of all river harvested clay catalysts. The hysteresis loop associated with the type-IV isotherm ensures pore condensation.[49] The kink in the desorption isotherm (Figure 3 (a–e)) attributed to desorption mode changes from capillary evaporation to multilayer desorption[50] which, indicates that the capillary nitrogen is almost absent in synthesized river clay catalysts.[51]

The calcination temperature significantly influenced the surface area of river harvested clay catalysts. The surface area of raw river harvested clay catalyst (RHC) was 1.25 m^2/g. This low surface area of RHC (1.25 m^2/g) was due to the less number of pores. However, as the calcination temperature increased from 600 °C to 800 °C, the surface area also increased i.e., surface area of 2.40 m^2/g for RHC-600, surface area of 7.62 m^2/g for RHC-700, and surface area of 18.83 m^2/g for RHC-800. Thus, the highest surface area was recorded for RHC-800 catalyst.

Whereas, the surface area of river harvested clay decreased to 5.74 m^2/g after calcination at a temperature of 900 °C. It may be due to the pore blockage or sintering phenomenon at very high calcination temperature of 900 °C. The BET surface area of river harvested clay catalysts are reported in the Table 2.

Fourier transform infrared (FTIR) analysis

The FTIR spectra of river harvested clay catalysts i.e., natural river harvested clay (RHC), river clay calcined at 600 °C (RHC-600), river clay calcined at 700 °C (RHC-700), river clay calcined at 800 °C (RHC-800) and river clay calcined at 900 °C (RHC-900) is given in

Table 1. EDX analysis of raw and calcined river harvested clay catalysts.

Catalyst type	EDX analysis					(Si/Al)
	O (wt.%)	Mg (wt.%)	Al (wt.%)	Si (wt.%)	Ca (wt.%)	
RHC	74.94	0.71	10.24	10.97	3.13	1.07
RHC-600	37.95	9.82	23.24	27.79	1.19	1.20
RHC-700	41.53	1.90	18.95	35.27	2.34	1.86
RHC-800	35.76	2.36	16.37	36.53	8.98	2.23
RHC-900	40.19	1.91	24.67	30.47	2.76	1.23

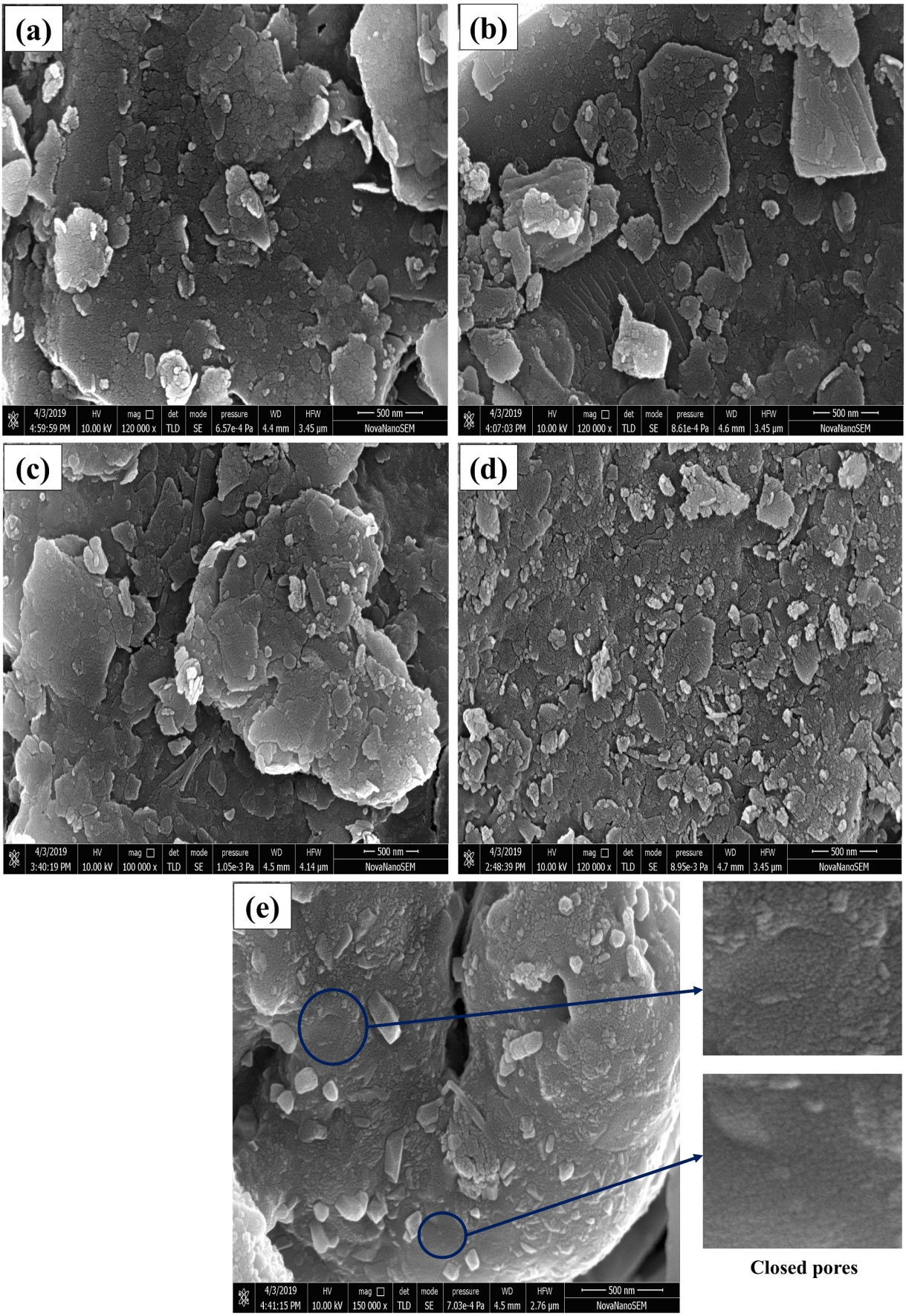

Figure 2. SEM images of river harvested clay catalyst (a) raw river clay (b) river clay calcined at 600 °C (c) river clay calcined at 700 °C (d) river clay calcined at 800 °C (e) river clay calcined at 900 °C.

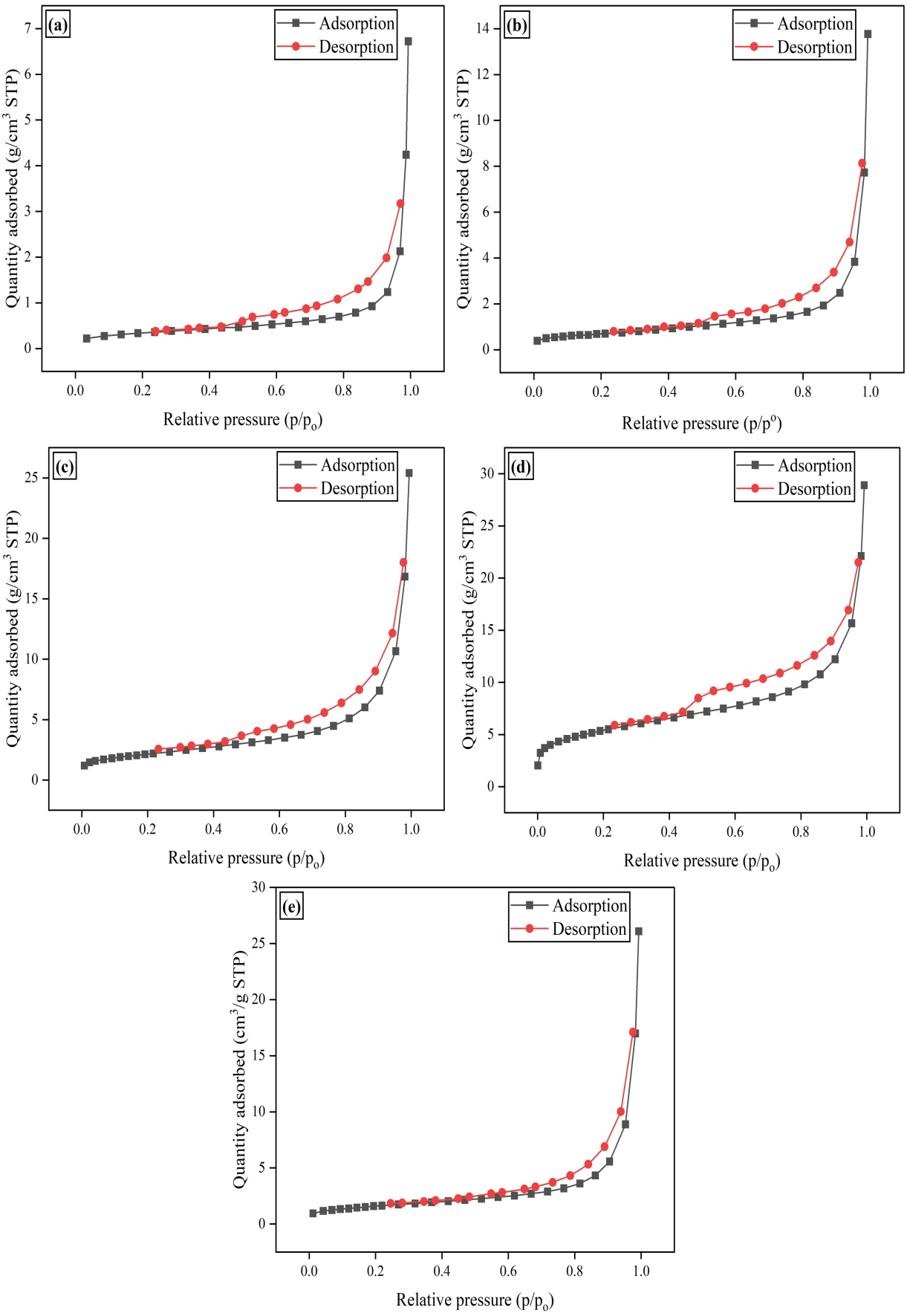

Figure 3. Nitrogen adsorption/desorption curve of river harvested clay catalyst (a) raw river clay (b) river clay calcined at 600 °C (c) river clay calcined at 700 °C (d) river clay calcined at 800 °C (e) river clay calcined at 900 °C.

Table 2. Surface area of river harvested clay catalysts at different calcination temperatures.

Catalyst type	BET surface area (m^2/g)
RHC	1.25
RHC-600	2.40
RHC-700	7.62
RHC-800	18.83
RHC-900	5.74

Figure 4. The broad band in the range between 3700 cm^{-1} to 3400 cm^{-1} includes the subsequent vibrations; (i) Si-OH, (ii) bridged hydroxyl groups in the form of Si-OH–Al and (iii) -OH hydroxyl groups.[52,53] Where, bridged -OH groups in the form of Si-OH–Al confirms the strong Bronsted acid sites.[53] The H-OH bending vibrations were noticed between the wavenumber of 1700 cm^{-1}–1400 cm^{-1} for the adsorbed water molecules.[28] The vibrations of the internal tetrahedral TO_4 (T=Si, Al) were observed between 1250 cm^{-1}–950 cm^{-1} and 720 cm^{-1}–650 cm^{-1} for asymmetric and symmetric stretching, respectively. Whereas, symmetric stretching of external linkage between tetrahedral units was

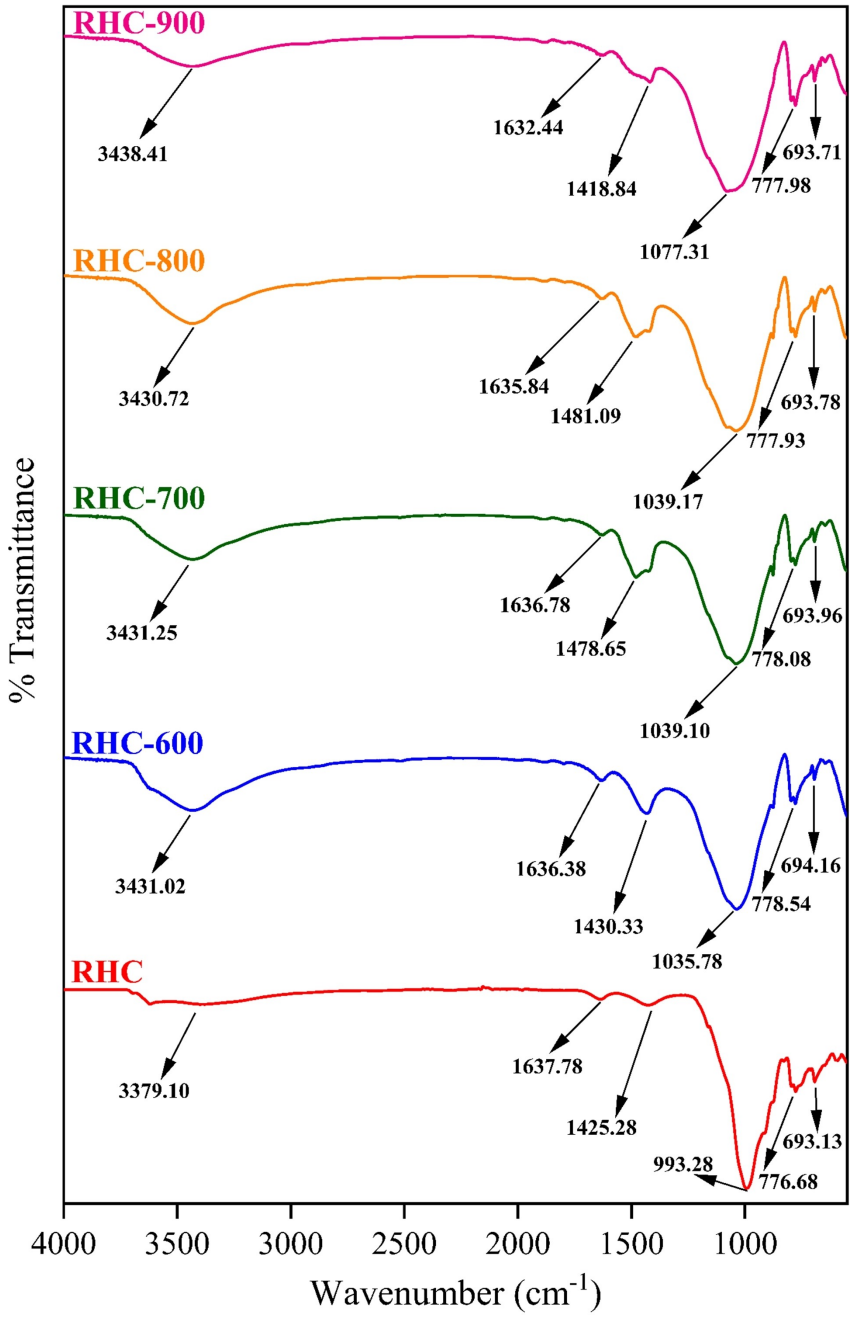

Figure 4. FTIR analysis of raw river harvested clay (RHC) catalyst and calcined river harvested clay catalysts i.e., river clay calcined at 600 °C (RHC-600), river clay calcined at 700 °C (RHC-700), river clay calcined at 800 °C (RHC-800), river clay calcined at 900 °C (RHC-900).

observed between 820 cm^{-1}–750 cm^{-1}.[54] All the observed peaks for the river clay catalysts are listed in Table S1.

Performance comparison of river harvested clay catalysts

The catalytic pyrolysis of WEPS was carried out using all types of synthesized river clay catalysts i.e., RHC, RHC-600, RHC-700, RHC-800 and RHC-900 for the selection of best river clay catalyst in terms of liquid yield, rich in BTE content. The Lp-type catalytic pyrolysis was conducted at a temperature of 600 °C. Whereas, Vp-type and Mp-type catalytic pyrolysis were conducted at a temperature of 550 °C. The heating rate of 15 °C/min and feed to catalyst ratio of 20:1 were maintained during the pyrolysis process. Table S2 shows the liquid yield of catalytic pyrolysis of WEPS using all types of river harvested clay catalysts along with their BTE and undesired styrene content.

It should be noted from Table S2 that the RHC-800 catalyst produced highest BTE content with low styrene as compared to the other river harvested clay catalysts, irrespective of all reactor arrangements. It may be due to the highest surface area (18.83 m^2/g) and high silica to alumina ratio (2.23) of RHC-800 catalyst, which provides higher active acidic sites for secondary reactions like cracking and hydrogenation. Furthermore, XRD analysis revealed that the, all possible transition alumina like kappa alumina, delta alumina, theta alumina were also found in the RHC-800 catalyst. In addition, FTIR analysis confirms the Bronsted acid sites in the RHC-800 catalyst, required for the formation of target molecules BTE. The BTE content of 21.06 wt.% was found in the pyrolysis oil obtained from liquid phase pyrolysis using RHC-800 catalyst. Whereas, the BTE content of 22.31 wt.% and 23.51 wt.% were found in the pyrolysis oil obtained from vapour phase and multiphase pyrolysis using RHC-800 catalyst. However, liquid yield obtained from RHC-800 catalyst for each reactor arrangement was slightly low as compared to the other catalysts. It is also attributed to the high surface area of RHC-800 catalyst which promotes the formation of gaseous range molecules. It is seen from Table S2 that the RHC-800 catalyst produced a maximum liquid yield of 89.75 wt.% at a temperature of 600 °C for liquid phase/Lp-type pyrolysis, 83.18 wt.% at a temperature of 550 °C for vapour phase/Vp-type and 81.93 wt.% at a temperature of 550 °C for multiphase/Mp-type pyrolysis. The quality of pyrolysis oil obtained using RHC-800 catalyst was found to be excellent in terms of BTE content as compared to the other catalysts. Even though the liquid yield obtained using RHC-800 catalyst was slightly low irrespective of reactor arrangement as compared to other catalysts. Thus, the RHC-800 catalyst was found to be the best catalyst among all other catalysts and used for further study.

Effect of parameters on pyrolysis products yieldEffect of catalyst amount

The liquid phase/Lp-type catalytic pyrolysis experiments were carried out by taking different feed to catalyst ratio in the range of 10:1–40:1, at a fixed pyrolysis temperature of 600 °C and heating rate of 15 °C/min to evaluate the optimum catalyst amount for producing the higher liquid yield. The product yields obtained at various feed to catalyst ratio produced from Lp-type pyrolysis using RHC-800 catalyst are mentioned in Table 3.

As the feed to catalyst ratio increased from 10:1 to 20:1, the liquid yield drastically increased from 83.54 wt.% to 89.75 wt.% (Table 3). Beyond the feed to catalyst ratio of 20:1, the liquid yield get decreases due to the lesser active sites of catalyst available for the cracking because of the higher amount of feed. The liquid yield of 86.97 wt.% and 84.68 wt.% were recorded at the feed to catalyst ratio of 30:1 and 40:1, respectively. The maximum liquid yield of 89.75 wt.% was recorded using feed to catalyst ratio of 20:1. It may be due to enough catalytic sites available for the interaction with the reactants. Although, at a low feed to catalyst ratio of 10:1, the reactant is insufficient to produce a high liquid yield because of higher catalyst active sites.[55]

Effect of heating rate

The effect of heating rate on the yield of pyrolysis products was investigated at different heating rates in the range of 5 °C/min - 25 °C/min, keeping reaction temperature fixed at 550 °C and using a fixed feed to catalyst ratio of 20:1. It is seen from Figure 5 that the liquid yield was observed to increase with the increase in heating rate up to 15 °C/min for each type of reactor arrangement. Beyond the heating rate of 15 °C/min, liquid yield decreases with the increase in heating rate. Thus, the maximum liquid yield for all types of reactor arrangement was recorded only at a heating rate of 15 °C/min due to the selective degradation of hydrocarbon molecules inside the reactor responsible for the formation of mainly liquid range hydrocarbon molecules.

The maximum liquid yield of 91.69 wt.%, 85.44 wt.%, 83.18 wt.% and 81.93 wt.% were obtained from thermal, Lp-type, Vp-type and Mp-type catalytic pyrolysis, respectively at a heating rate of 15 °C/min. The gaseous yield of 8.17 wt.%, 13.78 wt.%, 16.45 wt.% and 17.55 wt.% were obtained from thermal, Lp-type, Vp-type and Mp-type pyrolysis, respectively at a same heating rate of 15 °C/min as mentioned above. Lower liquid yields were recorded at low heating rates, such as 5 °C/min and 10 °C/min as compared to the heating rate of 15 °C/min. It may be due to the long residence time of molecules inside the reactor to attain its final designated temperature which, promotes the further cracking of molecules and is responsible for the high gaseous

Table 3. Product yield obtained from Lp-type catalytic pyrolysis at various feed to catalyst ratio.

Feed to catalyst ratio	Liquid (wt.%)	Gas (wt.%)	Solid (wt.%)
10:1	83.54	12.67	3.79
20:1	89.75	8.04	2.21
30:1	86.97	10.88	2.15
40:1	84.68	14.05	1.27

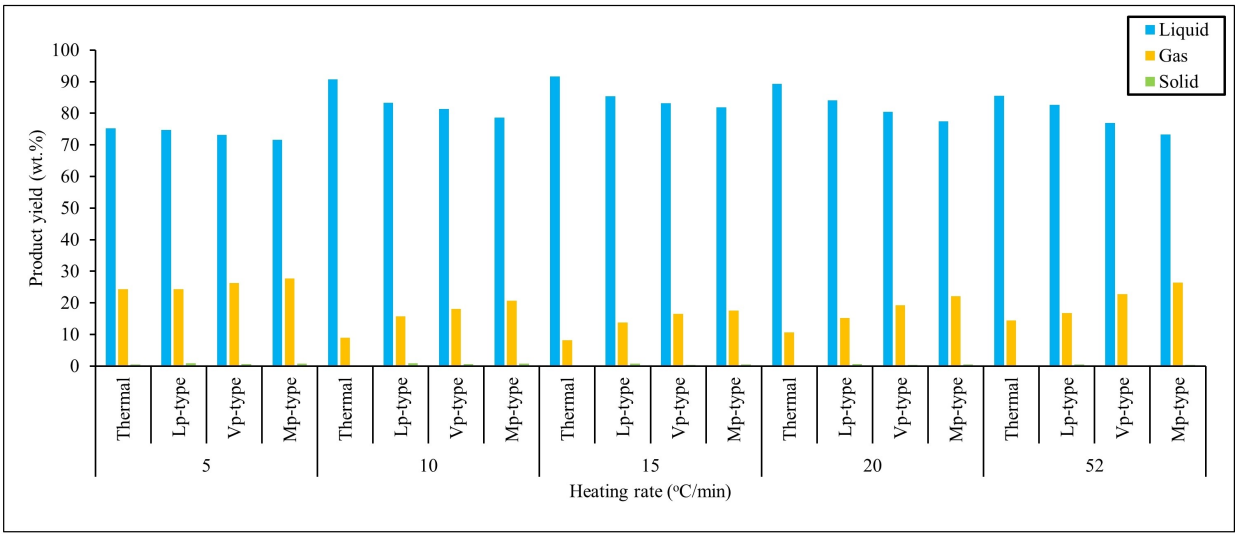

Figure 5. Effect of heating rate on product yield at a fixed reaction temperature of 550 °C and feed to catalyst ratio of 20:1.

yield and comparatively lower liquid yield. The liquid yield of 75.26 wt.%, 74.76 wt.%, 73.12 wt.% and 71.58 wt.% were obtained from thermal, Lp-type, Vp-type, and Mp-type catalytic pyrolysis, respectively at a heating rate of 5 °C/min. Interestingly, at higher heating rates, such as at 20 °C/min and 25 °C/min, lesser liquid yields were also observed for all types of pyrolysis. It may be due to the β-reaction mainly occurring at higher heating rates.[55] The liquid yield of 89.33 wt.%, 84.11 wt.%, 80.48 wt.% were obtained for thermal, Lp-type, Vp-type and Mp-type pyrolysis, respectively at a heating rate of 20 °C/min.

Effect of pyrolysis temperature

The influence of reaction temperature on the pyrolysis process yield was determined at different reaction temperatures ranging from 400 °C-700 °C. All other parameters such as heating rate (15 °C/min) and feed to catalyst ratio (20:1) were kept constant for studying the effect of temperature on the product yield. Figure 6 clearly shows that the liquid yield for thermal pyrolysis increases from 87.18 wt.% to 94.37 wt.% with an increase in reaction temperature from 400 °C to 650 °C. Beyond 650 °C, liquid yield get decreases due to the strong C–C cracking at the higher reaction temperature.[56] Thus, the maximum liquid yield of 94.37 wt.% was obtained from thermal pyrolysis with a gaseous yield of 5.55 wt.% at a reaction temperature of 650 °C. It should

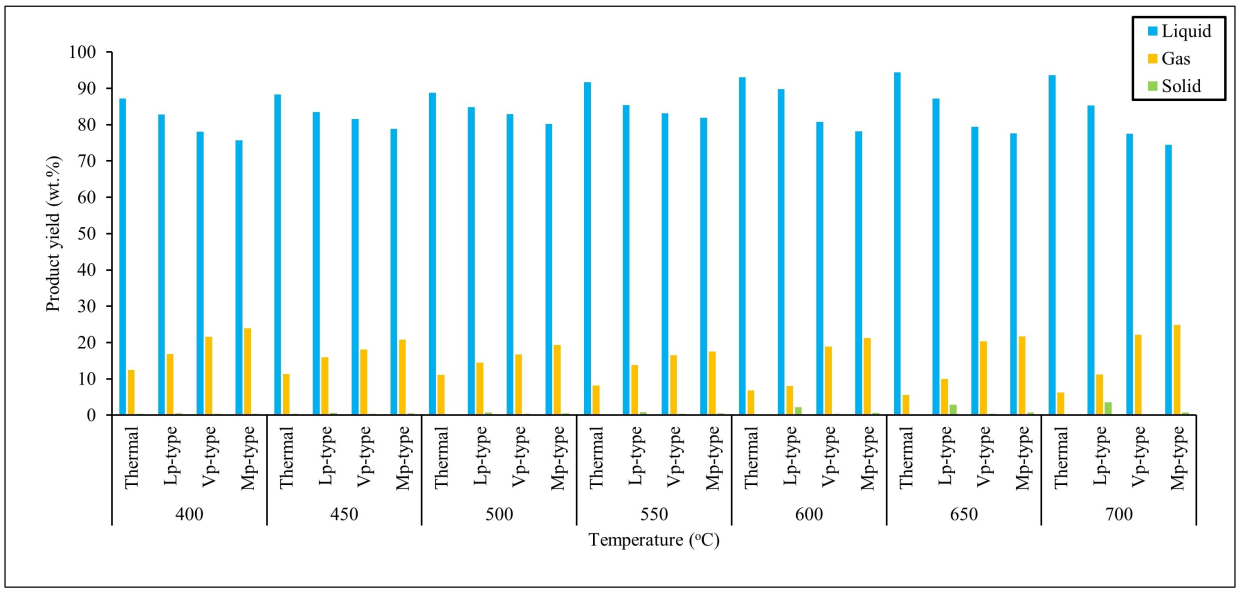

Figure 6. Effect of reaction temperature on the product yield at fixed heating rate of 15 °C/min and feed to catalyst ratio of 20:1.

be noted from Figure 6 that the catalytic pyrolysis of all types i.e., Lp-type, Vp-type and Mp-type using RHC-800 catalyst, always produced lesser liquid yield as compared to the thermal pyrolysis at each reaction temperature. This is because of catalyst improves the cracking and minimizes the required temperature for reaction by reducing the activation energy.[57] However, among all types of reactor arrangements, Mp-type/multiphase pyrolysis produced higher gaseous yield because of two stage catalytic cracking.

It is already mentioned in the experimental section, the multiphase reactor arrangement provides the two stage catalytic cracking i.e., first stage liquid phase cracking in the primary reactor and vapour phase catalytic cracking in the secondary reactor. The maximum liquid yield of 81.93 wt.% was obtained at a reaction temperature of 550 °C for Mp-type catalytic pyrolysis. Whereas, the gaseous yield of 17.55 wt.% was obtained for Mp-type pyrolysis at a temperature of 550 °C. Furthermore, Vp-type pyrolysis also offers two stage cracking i.e., first stage purely thermal cracking in the primary reactor and second-stage vapour phase catalytic cracking within the secondary reactor. Thus, Vp-type pyrolysis produced a slightly higher liquid yield as compared to the Mp-type pyrolysis. The maximum liquid yield of 83.18 wt.% and gaseous yield of 16.45 wt.% were obtained at a pyrolysis temperature of 550 °C for Vp-type pyrolysis. The Lp-type reactor arrangement facilitates only single-stage liquid phase catalytic cracking. Therefore, Lp-type pyrolysis produces a higher liquid yield at each reaction temperature compared to other types of catalytic pyrolysis. The maximum liquid yield of 89.75 wt.% and gaseous yield of 8.04 wt.% were recorded for the Lp-type pyrolysis at a reaction temperature of 600 °C. It should be noted that the maximum liquid yield of 94.37 wt.% at a temperature of 650 °C, 89.75 wt.% at a temperature of 600 °C and 83.18 wt.% at a reaction temperature of 550 °C and 81.93 wt.% at a reaction temperature of 550 °C for thermal, Lp-type, Vp-type and Mp-type pyrolysis, respectively as mentioned in Table 4.

Pyrolysis oil analysisDetermination of BTE content

The determination of BTE is directly associated with the quality of pyrolysis oil. As in the present research work, our aim is to minimize the styrene and increase the BTE content in the pyrolysis oil. However, styrene is also present in the pyrolysis oil which can be removed from the pyrolysis oil and stored separately for the production of other virgin resins. Upon styrene storage in a vessel during the summer, unwanted styrene dimers, trimers, or high molecular components are formed because of auto-polymerization. Thus, to prevent such autopolymerisation, addition of polymerization inhibitors should be added with styrene during storage.[58] In this context, the measurement of styrene is also important. The BTE content of pyrolysis oil was determined using calibration characteristics. The calibration characteristic curve was plotted between concentration (wt.%) of benzene, toluene, ethylbenzene and styrene versus % area (Figure S5). For plotting the calibration curve, highly pure HPLC grade benzene, toluene, ethylbenzene and styrene were mixed in different ratios and each mixture was analysed using GC to obtain the % peak area of each component for their known weight percent. The product yield, along with BTE and styrene content of pyrolysis oil obtained from thermal and catalytic pyrolysis at each pyrolysis temperature, is listed in Table S3. However, the BTE and styrene content of pyrolysis oil obtained at optimized conditions are listed in Table 5.

It should be noted from Table S3, that the highest BTE content was obtained at only optimum temperatures i.e., 650 °C for thermal pyrolysis, 600 °C for Lp-type, 550 °C for Vp-type and Mp-type catalytic pyrolysis using RHC-800 catalyst. The thermal pyrolysis oil mainly composed of styrene monomer (84.74 wt.%). Very less BTE content of 11.38 wt.% was reported for the thermal pyrolysis oil (Table 5). It is also reported in the open literature that the thermal pyrolysis of polystyrene mainly produced styrene monomer.[59] However, aromatization, cracking, oligomerization, isomerization, and alkylation reactions are responsible

Table 4. Product yield obtained from thermal and all types of catalytic pyrolysis at their respective optimum temperature and optimum heating rate of 15 °C/min and feed to catalyst ratio of 20:1.

Pyrolysis type	Optimum temperature (°C)	Liquid yield (wt.%)	Gaseous yield (wt.%)	Solid yield (wt.%)
Thermal	650	94.37	5.55	0.08
Lp-type	600	89.75	8.04	2.21
Vp-type	550	83.18	16.45	0.37
Mp-type	550	81.93	17.55	0.52

Table 5. Product yield and BTE content of pyrolysis oil obtained at optimum conditions for various reactor arrangements.

Pyrolysis type	Optimum temperature (°C)	Liquid (wt.%)	Gas (wt.%)	Benzene (wt.%)	Toluene (wt.%)	Ethylbenzene (wt.%)	Styrene (wt.%)	Total BTE (wt.%)
Thermal	650	94.37	5.55	0.62	10.21	0.55	84.74	11.38
Lp-type	600	89.75	8.04	1.03	15.37	4.66	67.63	21.06
Vp-type	550	83.18	16.45	1.17	16.02	5.12	65.59	22.31
Mp-type	550	81.93	17.55	1.20	16.70	5.61	65.30	23.51

for the formation of aromatic hydrocarbons while thermal degradation of polystyrene. Figure 7 shows the key reaction pathways for the formation of benzene, toluene, ethylbenzene and styrene during catalytic pyrolysis of WEPS.[39,53]

As mentioned in the Figure 7, protons from Bronsted acid sites of catalyst (RHC-800) can attack a mid-chain phenyl group either at position 1 (route 2) or position 2 (route-1). Protonation at the position-1 (route-2) results in the formation of secondary carbocation. However, protonation at position 2 (route-1) leads to the formation of a more stable tertiary carbocation. The tertiary carbocation produced by route 1 undergoes β-scission to form end chain primary carbocation and a stable polymer chain with benzyl end group. The end chain carbocation can further undergo β-scission to form styrene. The formation pathways of toluene and ethylbenzene involve protonation of the ultimate or penultimate phenyl group in position 1 of the polystyrene chain, respectively. Toluene is formed via β-scission, while ethylbenzene is formed via β-scission followed by intermolecular proton shift with another polymer or oligomer chain. Route 2 proceeds via β-scission of the secondary carbocation to form benzene.[53] This shows that the protonation of the polystyrene chain i.e., attack of protons from Bronsted acid sites of catalyst are mainly responsible for the formation of benzene, toluene and ethylbenzene (BTE). It is also reported in open literature that the Bronsted acid sites of the solid catalyst are mainly responsible for the BTE formation.[31] Furthermore, the presence of Bronsted acid sites in synthesized river clay catalyst RHC-800 is confirmed by the FTIR analysis which also ensured the formation of valuable aromatics BTE.

Interestingly, the highest BTE content of 23.51 wt.% (Table 5) was found to be highest for the Mp-type pyrolysis oil because of two-stage catalytic contact as mentioned earlier. Whereas, the second highest BTE content of 22.31 wt.% (Table 5) was found for the Vp-type catalytic pyrolysis oil because of pure thermal cracking in first stage and vapour phase catalytic cracking in the second stage. Thus, it could be concluded that the secondary reactor accelerates the secondary reaction, which favours the formation of BTE. The BTE content of 21.06 wt.% (Table 5) was found to be the lowest for the Lp-type catalytic pyrolysis oil among catalytic pyrolysis oil because of single-stage liquid phase catalytic cracking. Figure S6a depicts the comparison of GC-characteristics of thermal pyrolysis oil obtained at a reaction temperature of 650 °C, Lp-type pyrolysis oil obtained at a reaction temperature of 600 °C, Vp-type and Mp-type pyrolysis oil obtained at a reaction temperature of 550 °C, respectively. The peaks related to the benzene at a retention time of 1.74 min, toluene at a retention time of 3.16 min, ethylbenzene at a retention time of 4.97 min and styrene at a retention time of 5.55 min were highlighted with the marker. It is also clear from Figure S6a that the intensity of peaks related to target molecules benzene, toluene and ethylbenzene were found to be highest for the multiphase catalytic pyrolysis oil. Figure S6b shows the comparison of GC-characteristic of Mp-type pyrolysis oil obtained at a temperature of 550 °C, heating rate of 15 °C/min using feed to catalyst ratio of 20:1, with GC-characteristics of commercial

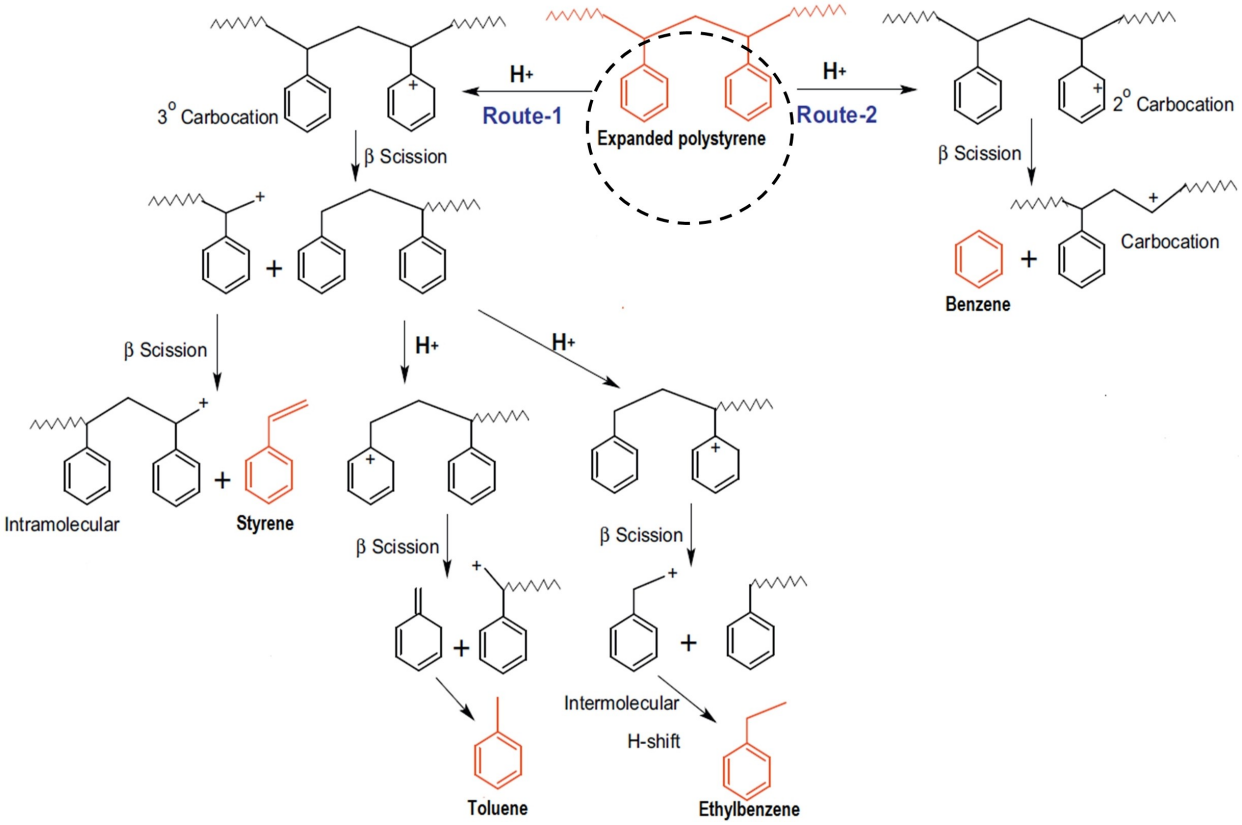

Figure 7. Reaction mechanism for the formation of BTE during catalytic pyrolysis.

fuels gasoline and kerosene. It should be noted from Figure S6b that the Mp-type catalytic pyrolysis oil also have components that are present in gasoline and kerosene at the higher retention time of 7.86 min, 9.67 min, 11.09 min and 13.39 min. However, gasoline and kerosene also contain benzene, toluene and ethylbenzene at the retention time of 1.74 min, 3.16 min, and 4.97 min, respectively.

Fourier transform infrared (FTIR) analysis

The FTIR spectra of pyrolysis oil obtained at a heating rate of 15 °C/min, feed to catalyst ratio of 20:1, and at temperature of 650 °C for thermal pyrolysis, 600 °C for Lp-type, 550 °C for Vp-type and Mp-type catalytic pyrolysis oil is mentioned in Figure S7. The functional groups observed in thermal and catalytic pyrolysis oil are listed in Table S4. The FTIR spectra confirm the presence of aromatic as well as aliphatic hydrocarbons in all types of pyrolysis oil. The peaks for aromatic C–H stretching were observed at a wavenumber of 3025.19 cm^{-1}, 3025.40 cm^{-1}, 3025.08 cm^{-1}, and 3025.32 cm^{-1} for thermal, Lp-type, Vp-type and Mp-type, respectively.[55] The methylene C–H asymmetric stretching vibrations were noticed at wavenumber of 2924.86 cm^{-1}, 2925.06 cm^{-1}, 2925.04 cm^{-1}, 2925.83 cm^{-1} for thermal, Lp-type, Vp-type and Mp-type, respectively. The vibrations for C=C–C aromatic ring stretching were detected at a wavenumber of 1600.45 cm^{-1}, 1599.47 cm^{-1}, 1600.23 cm^{-1} and 1598.25 cm^{-1} for thermal, Lp-type, Vp-type and Mp-type, respectively. The aromatic C–H in plane bending vibrations were observed at a wavenumber of 1072.04 cm^{-1}, 1076.17 cm^{-1}, 1075.94 cm^{-1} and 1075.00 cm^{-1} for thermal, Lp-type, Vp-type and Mp-type pyrolysis oil, respectively. Whereas, the vibrations for aromatic C–H out of plane bending were observed at a wavenumber of 777.54 cm^{-1}, 775.20 cm^{-1}, 775.63 cm^{-1}, 775.38 cm^{-1} for thermal, Lp-type, Vp-type and Mp-type pyrolysis oil, respectively. The cyclohexane ring vibrations were observed at a wavenumber of 1028.42 cm^{-1}, 1028.27 cm^{-1}, 1028.40 cm^{-1} and 1028.26 cm^{-1} for thermal, Lp-type, Vp-type and Mp-type pyrolysis oil, respectively.[60]

Physicochemical properties

The physicochemical properties i.e., higher heating value (HHV), flash point, fire point, and carbon residue of pyrolysis oil obtained at the optimum feed to catalyst ratio of 20:1, heating rate of 15 °C/min from all type of pyrolysis at their optimum temperature conditions i.e., 650 °C for thermal pyrolysis, 600 °C for Lp-type, 550 °C for Vp-type and Mp-type pyrolysis were determined and listed in Table S5. The fuel properties of pyrolysis oil were also compared with commercial gasoline and kerosene. The HHV of multiphase pyrolysis oil (11592 Cal/g) (Table S5) was highest among all types of pyrolysis oil, even higher than the HHV of gasoline (11315 Cal/g) and kerosene (11052 Cal/g).[61] The higher HHV of Mp-type pyrolysis oil is due to the presence of lighter and gasoline range hydrocarbons. Whereas, the HHV of thermal pyrolysis oil was found to be lowest (9816 Cal/g) (Table S5) due to the presence of long chain heavier hydrocarbon molecules.[62] The flash and fire point of Mp-type pyrolysis oil were found to be 50 °C and 54 °C, respectively (Table S5). The flash and fire point of Mp-type catalytic pyrolysis oil were higher than the gasoline[63] and closer to the kerosene.[64] It should be noted that fuels with high enough flash point are easy to handle during storage and transportation.[65] Similarly, the carbon residue of Mp-type pyrolysis oil was also comparable with the carbon residue of gasoline and kerosene.[66] The low carbon residue of Mp-type pyrolysis oil shows the lesser carbon deposition on hot surfaces.[67] Thus, pyrolysis oil obtained from Mp-type pyrolysis could be recommended for generator sets or cooking stoves.

Conclusions

The river harvested clay catalyst is successfully synthesized for the effective conversion of waste expanded polystyrene in a multiphase pyrolysis process. The natural catalyst RHC-800 undoubtedly reduces the cost of the entire pyrolysis process for the production of value added chemicals and aromatic hydrocarbons benzene, toluene and ethylbenzene (BTE). The highest BET surface area of 18.83 m^2/g and high silica to alumina (Si/Al) ratio of 2.23 makes RHC-800 a suitable catalyst for the pyrolysis process among all other synthesized river clay catalyst. The RHC-800 catalyst effectively enhances the BTE content (23.51 wt.%) in pyrolysis oil as compared to the thermal pyrolysis oil (11.38 wt.%). Furthermore, the secondary reactor offered more vapour phase contact between the catalyst particles and hydrocarbon vapours. The styrene content was found in lowest amount of 65.30 wt.% for multiphase/Mp-type catalytic pyrolysis. Very high HHV of Mp-type pyrolysis oil (11592 Cal/g) confirms the presence of lighter hydrocarbons. The multiphase catalytic pyrolysis oil can be used as fuel in generator sets, and cooking stoves or can be used as a source of useful commodity chemicals BTE.

Supporting Information Summary

The supporting information file contains materials and methods, catalyst synthesis, experimental set-up, characterization of catalyst and pyrolysis oil, EDX analysis of synthesized catalysts, calibration curve to determine the BTE and styrene content of pyrolysis oil, GC-characteristic of pyrolysis oil, FTIR spectra of pyrolysis oil, FTIR peaks for synthesized catalysts, Comparison between liquid yield and BTE content obtained from all synthesized catalysts, BTE content of pyrolysis oil obtained in the range of temperature 400 °C–700 °C, FTIR peaks for pyrolysis oil, and physicochemical properties of pyrolysis oil.

Acknowledgements

The authors have nothing to acknowledge for this submitted work.

Conflict of Interests

The authors declare that they have no known competing financial interests or personal relationships that could have appeared to influence the work reported in this research article.

Data Availability Statement

The data that support the findings of this study are available from the corresponding author upon reasonable request.

Keywords: BTE · Green catalyst · Multiphase pyrolysis · River harvested clay · Waste expanded polystyrene;

[1] J. Hopewell, R. Dvorak, E. Kosior, *Philos. Trans. R Soc. B: Biol. Sci.* **2009**, *364*, 2115.
[2] A. L. Andrady, M. A. Neal, *Philos. Trans. R Soc. B: Biol. Sci.* **2009**, *364*, 1977.
[3] P. Das, P. Tiwari, *Waste Manage.* **2018**, *79*, 615.
[4] P. Dwivedi, P. K. Mishra, M. K. Mondal, N. Srivastava, *Heliyon* **2019**, *5*, e02198.
[5] R. Miandad, M. A. Barakat, A. S. Aburiazaiza, M. Rehan, A. S. Nizami, *Process Saf. Environ. Prot.* **2016**, *102*, 822.
[6] K. Sun, Q. Huang, Y. Chi, J. Yan, *Waste Manage.* **2018**, *81*, 128.
[7] N. H. Ramli Sulong, S. A. Mustapa, M. K. Abdul Rashid, *J. Appl. Polym. Sci.* **2019**, *136*, 47529.
[8] C. Shin, *J. Colloid Interface Sci.* **2006**, *302*, 267.
[9] T. S. Hou, Y. S. Luo, *Geotech. Geol. Eng.* **2020**, *38*, 2539.
[10] Y. K. Song, S. H. Hong, S. Eo, G. M. Han, W. J. Shim, *Environ. Sci. Technol.* **2020**, *54*, 11191.
[11] Adnan, J. Shah, M. R. Jan, *J. Taiwan Inst. Chem. Eng.* **2014**, *45*, 2494.
[12] K. B. Park, S. J. Oh, G. Begum, J. S. Kim, *Energy* **2018**, *157*, 402.
[13] D. Czajczynska, L. Anguilano, H. Ghazal, R. Krzyzynska, A. J. Reynolds, N. Spencer, H. Jouhara, *Therm. Sci. Eng.* **2017**, *3*, 171.
[14] A. Adrados, I. De Marco, B. M. Caballero, A. Lopez, M. F. Laresgoiti, A. Torres, *Waste Manage.* **2012**, *32*, 826.
[15] J. Su, C. Fang, M. Yang, C. You, Q. Lin, X. Zhou, H. Li, *J. Anal. Appl. Pyrolysis* **2019**, *139*, 274.
[16] Y. Zhang, D. Duan, H. Lei, E. Villota, R. Ruan, *Appl. Energy* **2019**, *251*, 113337.
[17] K. Ding, S. Liu, Y. Huang, S. Liu, N. Zhou, P. Peng, Y. Wang, P. Chen, R. Ruan, *Energy Convers. Manage.* **2019**, *196*, 1316.
[18] A. Lopez, I. De Marco, B. M. Caballero, A. Adrados, M. F. Laresgoiti, *Waste Manage.* **2011**, *31*, 1852.
[19] A. Marcilla, A. Gomez-Siurana, D. Berenguer, *Appl. Catal. A* **2006**, *301*, 222.
[20] M. Olazar, G. Lopez, M. Amutio, G. Elordi, R. Aguado, J. Bilbao, *J. Anal. Appl. Pyrolysis* **2009**, *85*, 359.
[21] R. Bagri, P. T. Williams, *J. Anal. Appl. Pyrolysis* **2002**, *63*, 29.
[22] G. Elordi, M. Olazar, G. Lopez, M. Amutio, M. Artetxe, R. Aguado, J. Bilbao, *J. Anal. Appl. Pyrolysis* **2009**, *85*, 345.
[23] C. Kassargy, S. Awad, G. Burnens, K. Kahine, M. Tazerout, *Fuel* **2018**, *224*, 764.
[24] J. Zeaiter, *Fuel* **2014**, *133*, 276.
[25] N. Miskolczi, J. Sója, E. Tulok, *J. Anal. Appl. Pyrolysis* **2017**, *128*, 1.
[26] M. Benedetti, L. Cafiero, D. De Angelis, A. Dell'Era, M. Pasquali, S. Stendardo, R. Tuffi, S. V. Ciprioti, *Front. Environ. Sci. Eng.* **2017**, *11*, 1.
[27] K. T. Kyaw, C. S. Hmwe, *Int. J. Adv. Eng. Technol.* **2015**, *8*, 794.
[28] P. Gaurh, H. Pramanik, *Waste Manage.* **2018**, *77*, 114.
[29] J. Nisar, G. Ali, A. Shah, M. Iqbal, R. A. Khan, F. Anwar, R. Ullah, M. S. Akhter, *Waste Manage.* **2019**, *88*, 236.
[30] J. J. Park, K. Park, J. S. Kim, S. Maken, H. Song, H. Shin, J. W. Park, M. J. Choi, *Energy Fuels* **2003**, *17*, 1576.
[31] M. Marczewski, E. Kamińska, H. Marczewska, M. Godek, G. Rokicki, J. Sokołowski, *Appl. Catal. B.* **2013**, *129*, 236.
[32] D. G. Poduval, J. R. Van Veen, M. S. Rigutto, E. J. Hensen, *Chem. Commun.* **2010**, 3466.
[33] C. H. Zhou, *Appl. Clay Sci.* **2011**, *53*, 87.
[34] J. Wang, J. Jiang, Y. Sun, Z. Zhong, X. Wang, H. Xia, G. Liu, S. Pang, K. Wang, M. Li, J. Xu, *Energy Convers. Manage.* **2019**, *200*, 112088.
[35] E. Wijngaarden, P. A. Stewart, *Appl. Occup. Environ. Hyg.* **2003**, *18*, 678.
[36] Z. Ye, J. M. Giraudon, N. De Geyter, R. Morent, J. F. Lamonier, *Catalysts* **2018**, *8*, 91.
[37] W. Yang, Z. Wang, H. Sun, B. Zhang, *Chin. J. Catal.* **2016**, *37*, 16.
[38] F. A. Kuranchie, P. N. Angnunavuri, F. Attiogbe, E. N. Nerquaye-Tetteh, *Cogent. Environ. Sci.* **2019**, *5*, 1603418.
[39] A. Verma, S. Sharma, H. Pramanik, *Waste Manage.* **2021**, *120*, 330.
[40] R. R. Miller, R. Newhook, A. Poole, *Crit. Rev. Toxicol.* **1994**, *24*, S1.
[41] L. M. Wu, C. H. Zhou, J. Keeling, D. S. Tong, W. H. Yu, *Earth-Sci. Rev.* **2012**, *115*, 373.
[42] Y. Pei, P. Y. Chen, Table of key lines in X-ray powder diffraction patterns of minerals in clays and associated rocks, **1977**.
[43] G. Varga, *Epitoanyag* **2007**, *59*, 6.
[44] A. Nmiri, N. Hamdi, O. Yazoghli-Marzouk, M. Duc, E. Srasra, *J. Mater. Environ. Sci.* **2017**, *8*, 276.
[45] P. S. Santos, H. S. Santos, S. P. Toledo, *Mater. Res.* **2000**, *3*, 104.
[46] R. Castillo, R. Fernández, M. Antoni, K. Scrivener, A. Alujas, J. F. Martirena, *Rev. Ing. Constr.* **2010**, *25*, 329.
[47] Y. H. Seo, K. H. Lee, D. H. Shin, *J. Anal. Appl. Pyrolysis* **2003**, *70*, 383.
[48] H. Zaitan, D. Bianchi, O. Achak, T. Chafik, *J. Hazard. Mater.* **2008**, *153*, 852.
[49] A. Andoni, K. Xhaxhiu, K. R. Taraj, A. Çomo, *Asian J. Chem.* **2014**, *26*, 6833.
[50] M. A. Hernandez, F. Rojas, V. H. Lara, *J. Porous Mater.* **2000**, *7*, 443.
[51] I. Maruyama, G. Igarashi, Y. Nishioka, *Cem. Concr. Res.* **2015**, *73*, 158.
[52] W. Rondon, D. Freire, Z. de Benzo, A. B. Sifontes, Y. González, M. Valero, J. L. Brito, *Am. J. Anal. Chem.* **2013**, *4*, 584.
[53] D. K. Ojha, R. Vinu, *J. Anal. Appl. Pyrolysis* **2015**, *113*, 349.
[54] K. Byrappa, B. S. Kumar, *Asian J. Chem.* **2007**, *19*, 4933.
[55] A. Verma, S. Sharma, H. Pramanik, *Int. J. Energy Res.* **2022**, *46*, 15463.
[56] A. Lopez, I. De Marco, B. M. Caballero, M. F. Laresgoiti, A. Adrados, *Chem. Eng. J.* **2011**, *173*, 62.
[57] A. F. Anene, S. B. Fredriksen, K. A. Sætre, L. A. Tokheim, *Sustainability* **2018**, *10*, 3979.
[58] K. B. Park, Y. S. Jeong, B. Guzelciftci, J. S. Kim, *Appl. Energy* **2020**, *259*, 114240.
[59] D. S. Achilias, I. Kanellopoulou, P. Megalokonomos, E. Antonakou, A. A. Lappas, *Macromol. Mater. Eng.* **2007**, *292*: 923.
[60] Coates J. Interpretation of infrared spectra, a practical approach. Encyclopedia of Analytical Chemistry: Applications, Theory and Instrumentation. Chichester, UK: John Wiley & Sons; 2006. doi: 10.1002/9780470027318.a5606.
[61] P. Gaurh, H. Pramanik, *Int. J. Chem. Technol.* **2019**, *25*, 336.
[62] S. S. Lam, A. D. Russell, C. L. Lee, H. A. Chase, *Fuel* **2012**, *92*, 327.
[63] V. Mukhraiya, R. K. Yadav, B. Raikawar, *Int. J. Mech. Eng. Technol.* **2015**, *6*, 12.
[64] W. Ahmad, I. Ahmad, M. Ishaq, K. Ihsan, *Arab. J. Chem.* **2017**, *10*, S3263.
[65] A. P. Herrera, K. A. Ojeda, A. D. Penaloza, A. Rincón, *CT&F Cienc. Tecnol. Futuro* **2017**, *6*, 71.
[66] M. Shakirullah, W. Ahmad, I. Ahmad, M. Ishaq, *Fuel Process. Technol.* **2010**, *91*, 1736.
[67] P. T. Williams, R. P. Bottrill, A. M. Cunliffe, *Process Saf. Environ. Prot.* **1998**, *76*, 291.

Manuscript received: April 25, 2023